

## REFERENCES

1. A. J. Lowe, M. J. Powell, and S. R. Elliott, *J. Appl. Phys.*, **59**, 1251 (1986).
2. R. Hezel and N. Lieske, *ibid.*, **53**, 1671 (1982).
3. R. L. Pfeffer, G. J. Gerardi, R. A. Lux, K. A. Jones, E. H. Poindexter, W. H. Chang, and R. A. B. Devine, *Mat. Res. Soc. Symp. Proc.*, **165**, 227 (1990).
4. G. J. Valco, V. J. Kapoor, and M. D. Biedenbender, *This Journal*, **136**, 175 (1989).
5. S. Dzioba, S. Meikle, and R. W. Streater, *ibid.*, **134**, 2599 (1987).
6. G. Lucovsky, P. D. Richard, D. V. Tsu, S. Y. Lin, and R. J. Markunas, *J. Vac. Sci. Technol.*, **A4**, 681 (1986).
7. G. Lucovsky and D. V. Tsu, *ibid.*, **A5**, 2231 (1987).
8. S. V. Hattangady, G. G. Fountain, R. A. Rudder, and R. J. Markunas, *ibid.*, **A7**, 570 (1989).
9. D. V. Tsu and G. Lucovsky, *ibid.*, **A4**, 480 (1986).
10. R. Padmanabhan and N. C. Saha, *ibid.*, **A6**, 2226 (1988).
11. T. Hirao, K. Setsune, M. Kitagawa, T. Kamada, K. Wasa, and T. Izumi, *Jpn. J. Appl. Phys.*, **26**, 2015 (1987).
12. S. V. Nguyen and K. Albaugh, *This Journal*, **136**, 2835 (1989).
13. J. Dupuie and E. Gulari, *Appl. Phys. Lett.*, **59**, 549 (1991).
14. Y. Hirose and Y. Terasawa, *Jpn. J. Appl. Phys.*, **25**, L519 (1986).
15. S. Matsumoto, Y. Sato, M. Kamo, and N. Setaka, *ibid.*, **21**, L183 (1982).
16. A. Sawabe and T. Inuzuka, *Appl. Phys. Lett.*, **46**, 146 (1985).
17. H. Matsumura, *Jpn. J. Appl. Phys.*, **25**, L183 (1982).
18. K. Yasui, H. Katoh, K. Komaki, and S. Kaneda, *Appl. Phys. Lett.*, **56**, 898 (1990).
19. H. Matsumura, *Mat. Res. Soc. Symp. Proc.*, **118**, 43 (1988).
20. W. A. Lanford and M. J. Rand, *J. Appl. Phys.*, **49**, 2473 (1978).
21. S. Wolf and R. N. Tauber, "Silicon Processing for the VLSI Era, Volume 1—Process Technology," p. 193, Lattice Press, Sunset Beach, CA (1987).
22. C. D. Wagner, D. E. Passoja, H. F. Hillery, T. G. Kinisky, H. A. Six, W. T. Jansen, and J. A. Taylor, *J. Vac. Sci. Technol.*, **21**, 933 (1982).
23. J. A. Taylor, *Appl. Surf. Sci.*, **7**, 168 (1981).
24. D. Briggs and M. P. Seah, "Practical Surface Analysis by Auger and X-ray Photoelectron Spectroscopy," Ch. 4, John Wiley & Sons, New York (1984).
25. H. H. Andersen, *Appl. Phys.*, **18**, 131 (1979).
26. D. E. Aspnes and J. B. Theeten, *J. Appl. Phys.*, **50**, 4928 (1979).
27. H. R. Phillip, *This Journal*, **120**, 295 (1973).
28. M. L. Naiman, C. T. Kirk, B. L. Emerson, J. B. Taitel, and S. D. Senturia, *J. Appl. Phys.*, **58**, 779 (1985).
29. F. Terry, Private communication.
30. D. Stroud, *Phys. Rev.*, **B12**, 3368 (1975).
31. F. H. P. M. Habraken, A. E. T. Kuiper, A. v. Oostrom, Y. Tamminga, and J. B. Theeten, *J. Appl. Phys.*, **53**, 404 (1982).
32. H. D. Batha and E. D. Whitney, *J. Amer. Ceram. Soc.*, **56**, 365 (1973).
33. M. Grosman and D. G. Loffler, *J. Catal.*, **80**, 188 (1983).
34. G. S. Selwyn and M. C. Lin, *J. Chem. Phys.*, **67**, 213 (1982).
35. G. S. Selwyn, G. T. Fujimoto, and M. C. Lin, *J. Phys. Chem.*, **86**, 760 (1982).
36. S. N. Foner and R. L. Hudson, *J. Chem. Phys.*, **80**, 4013 (1984).
37. J. W. Sutherland and J. V. Michael, *ibid.*, **88**, 830 (1988).
38. J. E. Dove and W. S. Nip, *Can. J. Chem.*, **57**, 689 (1979).
39. D. F. Davidson, K. Kohse-Hoinghaus, A. Y. Chang, and R. K. Hanson, *Int. J. Chem. Kin.*, **22**, 513 (1990).
40. D. V. Tsu, G. Lucovsky, and M. J. Mantini, *Phys. Rev.*, **B33**, 7069 (1986).
41. G. Lucovsky, J. Yang, S. S. Chao, J. E. Tyler, and W. Czubatyj, *ibid.*, **B28**, 3234 (1983).

# Plasma Enhanced Chemical Vapor Deposition of Blanket $\text{TiSi}_2$ on Oxide Patterned Wafers

## I. Growth of Silicide

Jaegab Lee and Rafael Reif

Massachusetts Institute of Technology, Cambridge, Massachusetts 02139

### ABSTRACT

We investigated the effects of deposition variables on the growth of stable  $\text{TiSi}_2$  films and the silicon consumption from the substrate during the deposition of  $\text{TiSi}_2$  in a cold wall plasma enhanced chemical vapor deposition system. Low resistivity silicide films were deposited at temperatures ranging from 590 to 775°C and a  $\text{SiH}_4/\text{TiCl}_4$  flow rate from 6/2 to 10/6 (sccm). The as-deposited films did not require any postannealing to lower the resistivity. It was observed that, depending on deposition conditions, substrate silicon consumption occurred during silicide deposition. However, a high  $\text{SiH}_4$  flow rate and low deposition temperature effectively suppressed silicon consumption. The deposition of a conformal blanket  $\text{TiSi}_2$  film with no silicon consumption at 590°C and  $\text{SiH}_4/\text{TiCl}_4$  of 8/4 (sccm) confirmed the effects of temperature and gas flow ratio on silicon consumption. A kinetic model of silicon consumption is proposed to provide a description of the effects of silane gas flow rate on silicon consumption.

Refractory metal silicides have been used as interconnection and gate materials instead of, or in conjunction with, polycrystalline silicon to realize faster and smaller devices. Among the refractory metal silicides, titanium silicide has received much attention due to its lowest resistivity and its lower contact resistance as compared with the Al/Si contact structure (1). Recently, low pressure chemical vapor deposition (LPCVD) of titanium disilicide has been investigated as a means to deposit gate and interconnect silicide on  $\text{SiO}_2$  or silicon (2, 3). However, LPCVD of  $\text{TiSi}_2$  occurs in a narrow deposition window (4, 5), and a systematic investigation of the effects of deposition variables on the growth of the silicide is difficult to carry out.

In addition, LPCVD of  $\text{TiSi}_2$  experiences severe difficulties in controlling excessive silicon consumption (6, 7) with the rough interface of the resulting films, and nucleation problems due to the presence of the native oxide (8). Silicon consumption is expected to be a strong function of the deposition temperature and the  $\text{SiH}_4/\text{TiCl}_4$  flow rate ratios.

Plasma enhanced chemical vapor deposition (PECVD) enlarges the deposition variable window, especially the deposition temperature, thus enabling a better control of the process. By utilizing the large deposition variable space available with PECVD, we have studied the effects of deposition variables on the growth of silicide films and

silicon consumption. A kinetic model of silicon consumption is proposed to explain how the  $\text{SiH}_4$  gas flow rate affects silicon consumption. In addition, the thermodynamically possible reactions based on the by-product gases detected by a quadrupole mass spectrometer (QMS) are discussed to explain the effects of experimental variables on the deposition of the silicide.

In Part II (II. Silicide Properties) (7), the effect of deposition parameters on the material properties of as-deposited silicide films such as resistivity, surface morphology, structure, and composition is reported. In addition, a PECVD polycide structure was realized and the thermal stability of  $\text{TiSi}_2$  on  $\text{SiO}_2$  at  $950^\circ\text{C}$  was investigated to explore its application as a gate electrode material.

We modified a high vacuum, cold wall CVD reactor to incorporate plasma for the deposition of silicide films as well as for *in situ* surface cleaning prior to deposition.

### Deposition System

The schematic of the PECVD system used in this work is shown in Fig. 1. A turbomolecular pump, with a pumping speed of 500 l/s, is used to obtain a base pressure of  $<1 \times 10^{-7}$  Torr with the gate valve open.  $\text{SiH}_4$  and  $\text{TiCl}_4$  were used as the silicon and titanium sources, respectively.

The flow of gases in the reactor is controlled by mass flow controllers. A mass flow controller (MKS) of  $\text{TiCl}_4$  was specially designed to avoid the need for a carrier gas to deliver  $\text{TiCl}_4$  into the chamber and to avoid a surge of gas flow at the opening of the valve. However, a sudden increase in the  $\text{TiCl}_4$  flow at the opening of the valve to the chamber was observed. This initial surge of  $\text{TiCl}_4$  flow influenced initial deposition conditions, thereby resulting in lack of reproducibility. Therefore, a bypass line from the mass flow controller to a cold trap was installed to prevent the surge of the gas flow. A quadrupole mass spectrometer connected to the back side of the chamber was used for detecting by-product-gases, as well as for monitoring the tightness of the system. The pressure inside the chamber was monitored by a capacitance manometer during deposition.

During silicide deposition, the gate valve was closed and a pressure control arm was used as a pumping line to install a cold trap ( $-70^\circ\text{C}$ ) in the line. Unreacted  $\text{TiCl}_x$  gases condense on the inner tube of the cold trap, preventing their attacking of the turbopump. However,  $\text{HCl}$  generated in the system seems to pass through the cold trap, attacking the bearings of the turbopump.

The temperature of a single wafer sitting on a four-pin quartz holder was monitored by an infrared pyrometer through a sapphire window. A bank of 6 infrared lamps was designed to heat a single wafer directly utilizing maximum electrical power effectively, which facilitated abrupt changes in the wafer temperature. This was desirable to

quickly switch from *in situ* plasma cleaning at  $650^\circ\text{C}$  to a different deposition temperature.

The RF power supply was a 500 W, 13.56 MHz generator coupled through an automatic matching network to a 14 cm diam power electrode spaced 20 cm apart from the ground electrode. The wafer sitting on the quartz susceptor was electrically isolated. The plasma allowed *in situ* hydrogen plasma clean prior to a titanium silicide deposition as well as a plasma deposition of silicide. The electrical isolation of the wafer being in contact with the plasma allows a high flux of reactive radicals to the wafer surface under conditions of minimal ion bombardment, which favors the formation of a stable titanium disilicide.

### Experimental

Depositions were carried out on 100 mm, n-type,  $2.5 \Omega\text{-cm}$ , (100) silicon wafers under the conditions summarized in Table I. Wafers with a 100 or 500 nm thermally grown oxide were patterned. The oxide patterned wafers were cleaned in an RCA procedure followed by dipping into a 50:1 HF solution to remove the native oxide prior to loading. The wafers were rinsed, dried, and placed in the ultraviolet (UV)/ozone cleaning system to grow a passivating oxide (9). The clean wafer was moved directly from the ozone system into the chamber. After loading the wafer, the chamber was pumped down to a base pressure of  $1 \times 10^{-7}$  Torr. The wafer was then heated to deposition temperature and the chamber baked in argon to achieve a "hot" base pressure of  $5 \times 10^{-7}$  Torr. While baking the system, the cold trap was installed along the pressure control arm. The deposition procedure consisted of an *in situ* hydrogen plasma clean followed by a PECVD step. Bypass lines were used to stabilize the flow of gases before introducing the gases into the chamber. The deposition was initiated by striking a plasma after the  $\text{TiCl}_4$  and  $\text{SiH}_4$  gas flow stabilized into the chamber.

In this research, one of the goals was to determine the limiting step to silicon consumption to facilitate its suppression. Since a native oxide is thermodynamically stable up to high temperatures and also acts as a barrier layer to silicon diffusion, a clean silicon surface is necessary to study the dependence of silicon consumption on deposition variables. In our system, pure hydrogen plasma was used to remove the UV/ozone oxide prior to deposition. Removing the UV/ozone oxide ( $\sim 15 \text{ \AA}$ ) was expected to leave the silicon surface relatively free of impurities such as oxygen and carbon (10). The hydrogen plasma cleaning was done under the following conditions:  $\text{H}_2$  flow rate of 30 sccm, total pressure of 55 mTorr, substrate temperature of  $650^\circ\text{C}$ , duration time of 40 min, and input power of 15 W. This condition was identified to be effective to clean the surface prior to deposition of silicide. Any damage on the surface was not observed under scanning electron microscopy (SEM) and cross-sectional transmission electron microscopy (XTEM). Two samples were prepared under the same deposition conditions: one was exposed to UV-ozone in the UV-system, followed directly by deposition of  $\text{TiSi}_2$  in the reactor; the other was exposed to UV-ozone, followed by the  $\text{H}_2$  plasma cleaning prior to deposition of  $\text{TiSi}_2$ . Figure 2(a) shows that for the sample without plasma cleaning, the  $\text{TiSi}_2$  film in some surface areas ruptures the interface and grows into the silicon substrate. The rupture of the UVOC oxide is shown in Fig. 2(b). In the sample with plasma cleaning, the silicide is recessed into the silicon substrate, showing significant silicon consumption (see Fig. 2(c)). This difference between the two samples in

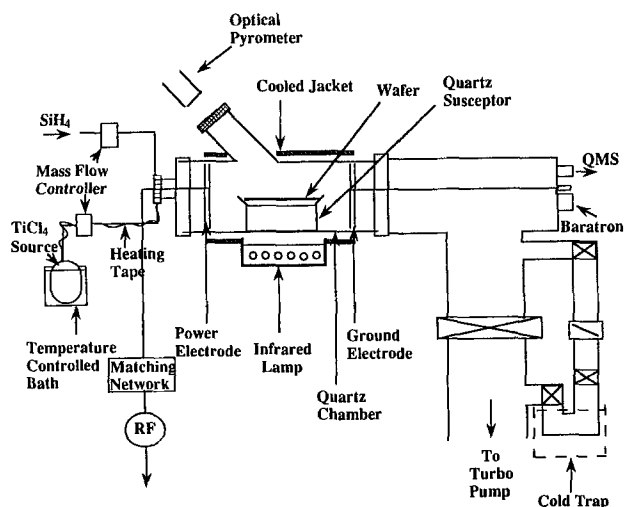


Fig. 1. Schematic of the PECVD titanium silicide reactor.

Table I. Deposition conditions.

	$\text{H}_2$ plasma	Titanium silicide
Temperature ( $^\circ\text{C}$ )	650	550-780
$\text{SiH}_4$ flow (sccm)		5-10
$\text{TiCl}_4$ flow (sccm)		2-7
$\text{H}_2$ flow (sccm)	30	5-30
Argon flow (sccm)		5-15
Pressure (mTorr)	55	37-83
Deposition time (min)	40	1-10
Power (W)	15	5

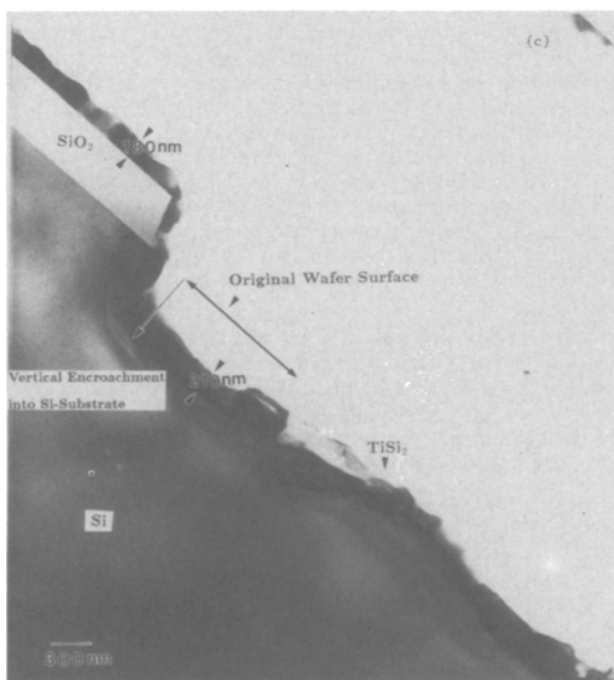
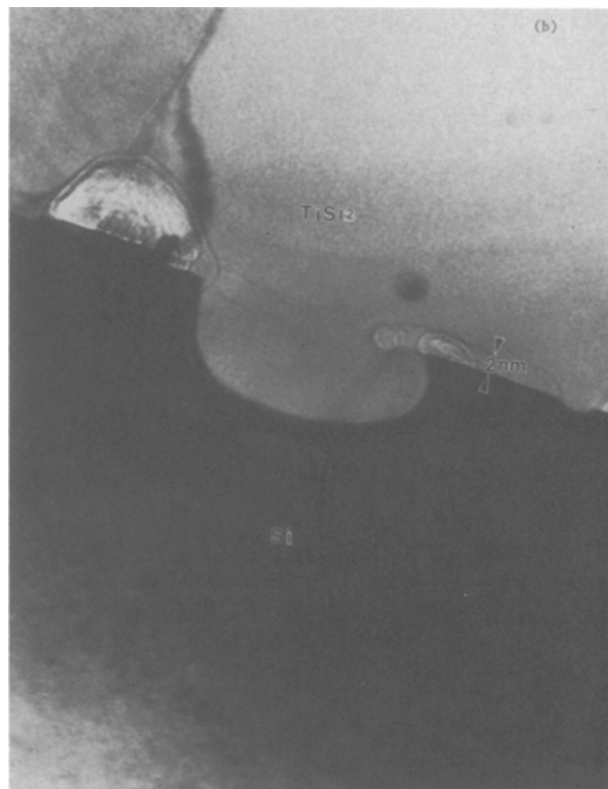
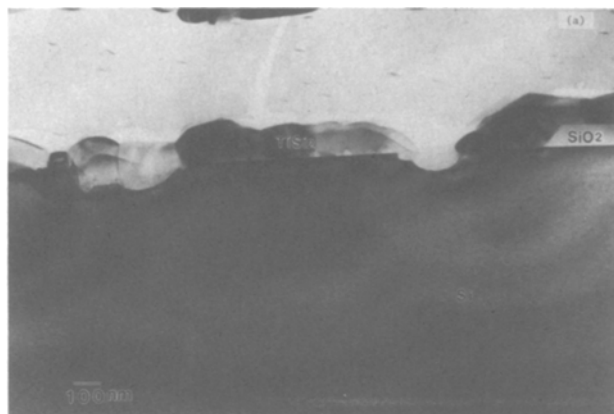


Fig. 2. Cross-sectional TEM of titanium silicide films deposited without  $H_2$  plasma cleaning, (a and b), and with  $H_2$  plasma cleaning, (c), prior to deposition of silicide deposited at  $650^\circ C$ , a  $SiH_4/TiCl_4$  flow rate ratio of 6/4 (sccm), a power of 5 W, and a duration time of 3 min.

the location of the interface between  $TiSi_2$  and silicon shows clearly that the hydrogen plasma effectively removed the passivating oxide under the stated conditions. The presence of the UV/ozone oxide layer seemed to block silicon diffusion into the silicide, but was not stable with respect to  $TiSi_2$  film, thereby leading to the rupture of the oxide. It is not yet clear what mechanism, *i.e.* the exothermic reaction of  $TiSi_2$  formation or the driving force for a reduction of  $SiO_2$  surface area, caused the rupture of the oxide. In addition to its use in the above comparison,  $H_2$  plasma cleaning was successfully used to deposit  $TiSi_2$  selectively on oxide patterned wafers around  $750^\circ C$ .

$TiSi_2$  film thicknesses were measured using a surface profilometer. XTEM was used to assess the crystalline quality of silicide films, the consumption of the silicon

substrate, and the grain size of a silicide film. Glancing angle x-ray diffractometry was used to determine the phases and the preferred orientation of the deposited films. SEM was used to study the surface morphology and Auger electron spectroscopy (AES) was used to detect impurities such as carbon and oxygen in the silicide films. Rutherford backscattering spectroscopy (RBS) spectra taken using 2 or 3 MeV  $He^{++}$  at normal incidence and  $4^\circ$  scattering angle determined the stoichiometry of the films. The sheet resistance of the silicide was measured using a four point probe.

### Results and Discussion

**Growth rate.**—Growth rate experiments were conducted at different temperatures, times, gas flow rate ratios, and

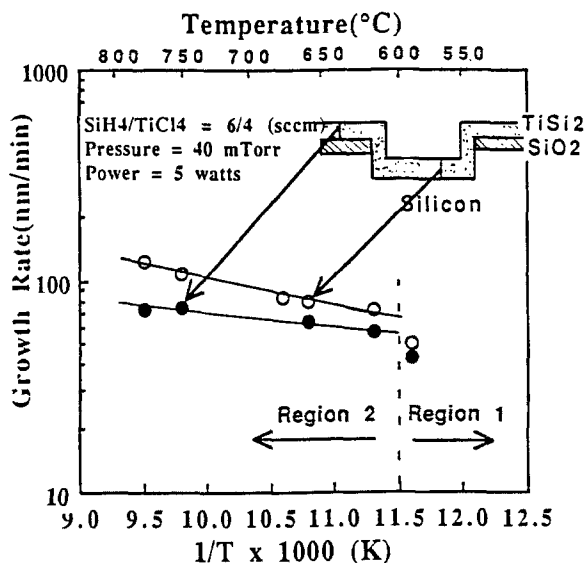


Fig. 3. Arrhenius plot of the growth rate of titanium silicides deposited on silicon and  $\text{SiO}_2$  for deposition conditions of  $\text{SiH}_4/\text{TiCl}_4$  flow rate ratio of 6/4 (sccm),  $650^\circ\text{C}$ , 40 mTorr, 3 min, and 5 W.

dilution gas (Ar or  $\text{H}_2$ ) flow rates. Typical duration times were 3 min. Figure 3 shows the growth rate of titanium silicide deposited on silicon window (open circle) and on silicon dioxide (closed circle) as a function of temperature. As the data show, for both substrates, there are two distinct regions of deposition rates. Region 2, at the higher temperatures, is only slightly temperature activated. At the lower temperatures (Region 1), the growth rate shows a strong temperature activation. In an attempt to reduce the effects of temperature variation on silicide growth rate, the dependence of the growth rate on duration times, gas flow rate ratios, and dilution gas flow rates was investigated at the constant temperature of  $650^\circ\text{C}$  (Region 2). According to CVD theory, Region 2 can be defined as mass transport limited and Region 1 as surface reaction limited.

At  $570^\circ\text{C}$ , no deposition of silicide occurred and several tiny etch pits were found scattered on the surface. As the temperature was increased to  $590^\circ\text{C}$ , the deposition started to take place. In the temperature range of  $580$  to  $600^\circ\text{C}$ , the reaction rate seems to be limited by surface kinetics on the substrate. As the deposition temperature was increased above  $600^\circ\text{C}$ , the difference in the growth rates of silicide between on silicon and on  $\text{SiO}_2$  increases. This indicates that, in the growth of silicide on silicon, increasing the temperature results in more silicon supplied from the substrate participating in the silicide formation.

Figure 4 shows the thickness of the silicide deposited both on silicon and on  $\text{SiO}_2$  as a function of time. The error bars in the thickness of silicide are partly due to the surface roughness and partly due to the interface roughness. As shown in Fig. 4, the growth rate of silicide appears to be constant with time. This suggests that  $\text{TiSi}_2$  growth is limited by the transport of gases ( $\text{TiCl}_4$  and/or  $\text{SiH}_4$ ) to the surface.

The effects of the gas flow rate of argon and hydrogen on the growth rate at  $650^\circ\text{C}$  is shown in Fig. 5. Both dilution gases decrease the growth rate of silicide with increasing flow rate. X-ray spectra reveal different effects of the two diluents on the preferred orientation of the silicide films. Hydrogen enhances the formation of randomly oriented grains, while argon does not change the orientation of grains. Therefore, the two dilution gases are expected to decrease the growth rate by influencing the reaction paths, such as mass transport of gases and surface reaction of adsorbed gases, in different ways in temperature Region 2.

Figure 6 shows the effects of silane gas flow rate on the thickness of silicide on silicon dioxide. As the  $\text{SiH}_4$  flow rate increases, the thickness of the silicide increases and reaches a maximum value at a  $\text{SiH}_4$  flow of 6 sccm, then it decreases. According to Fig. 3, the mass transfer of active radicals to the surface limits the growth of the silicide at

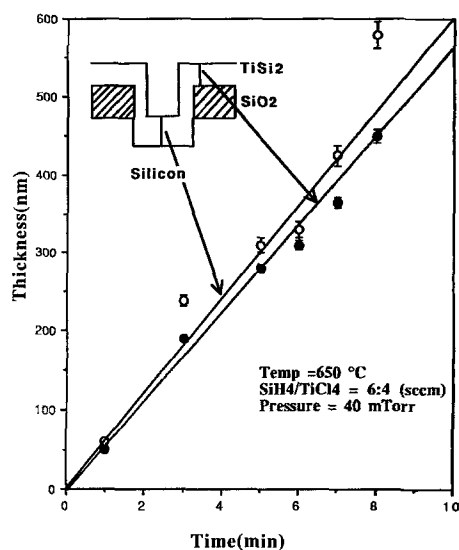


Fig. 4. The thickness of  $\text{TiSi}_2$  films deposited on silicon and on  $\text{SiO}_2$ , respectively, as a function of time, for deposition conditions of 6/4 (sccm),  $650^\circ\text{C}$ , 40 mTorr, and 5 W.

$650^\circ\text{C}$ . Therefore, local equilibrium may be assumed to exist between the adsorbed species and the gas species. Consequently, increasing the silane gas may reduce the concentration of adsorbed  $\text{TiCl}_x$  radicals leading to the decrease in the growth rate if  $\text{TiCl}_x$  species limit the growth.

The effects of  $\text{TiCl}_4$  gas flow rate on the growth rate is shown in Fig. 7. As the  $\text{TiCl}_4$  gas flow rate increases, the growth rate also increases, reaches a plateau, and then decreases. The decrease in the growth rate may be partly due to the reduced concentration of  $\text{SiH}_x$  radicals on the surface and partly due to the etching of the silicide which may occur with high chlorine concentrations (11). However, the evidence of etching of the silicide was not observed under SEM. The surface of silicide deposited on  $\text{SiO}_2$  was usually smooth. Therefore, according to Fig. 6 and Fig. 7, both reactants ( $\text{TiCl}_4$  and  $\text{SiH}_4$ ) seemed to be limiting sources to silicide formation so that the maximum growth rate was obtained at the optimum gas ratios in the temperature Region 2.

**Silicon consumption.**—Figure 2(c) reveals the silicide deposited on a  $\text{SiO}_2$  patterned wafer at  $650^\circ\text{C}$ , for 3 min, showing a uniform thickness on silicon as well as  $\text{SiO}_2$ . Excessive silicon consumption (3000 to 6000 Å) was observed to result in the vertical encroachment into the silicon substrate, especially at the base of the contact cut. This verti-

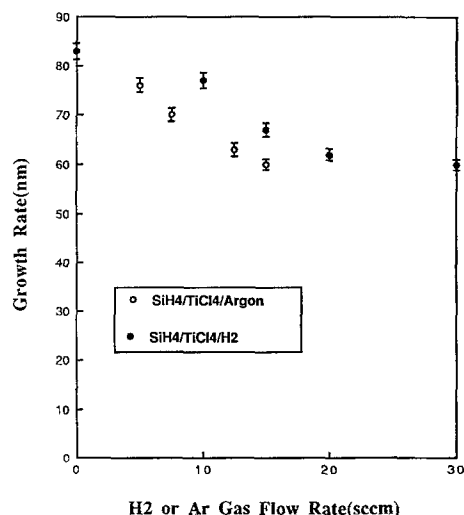


Fig. 5. The effects of (a)  $\text{H}_2$  and (b) Ar gas flow rates on the growth rate of silicide deposited on silicon with deposition conditions of  $\text{SiH}_4/\text{TiCl}_4$  of 6/4 (sccm),  $650^\circ\text{C}$ , and 5 W.

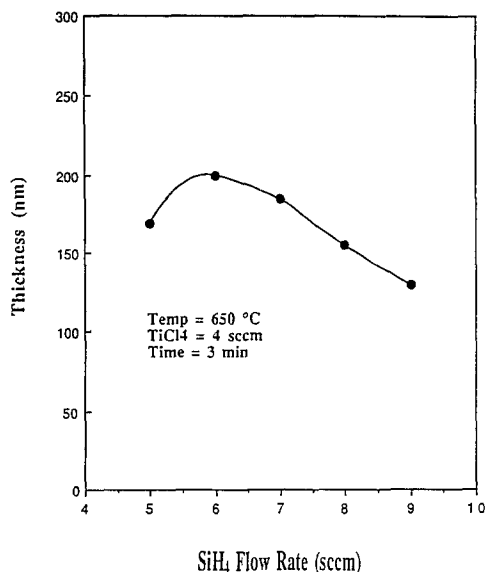


Fig. 6. The thickness of TiSi<sub>2</sub> deposited on SiO<sub>2</sub> as a function of SiH<sub>4</sub> flow rate for 3 min, at a TiCl<sub>4</sub> flow of 4 sccm, 650°C, and 5 W.

cal encroachment at the base of the contact window in Fig. 2(c) corresponds to the rough surface at the edge of the silicon window shown in Fig. 8(a). In addition, the surface morphology of silicide on SiO<sub>2</sub> is smooth, while that of silicide on silicon is rough (see Fig. 8). These observations suggest that the surface roughness on silicon is not caused by the etching of the silicide, but by nonuniform silicon consumption as well as silicon etching. In addition, the small difference (200 to 1000 Å) in the thickness of silicide on silicon and on SiO<sub>2</sub> cannot be explained by the large amount of silicon consumed (3000 to 6000 Å) if solid silicon is assumed to be a main contributor to silicide formation. Therefore, it is expected that a large fraction of silicon diffuses through the silicide layer and is etched away at the surface, while only a small fraction of silicon participates in silicide formation. Consequently, the silicon from the silane gas can be the main contributor to silicide formation. This fact is consistent with the constant growth rate in Fig. 4 and the observation of the maximum growth rate at the optimum gas ratios in Fig. 6 and Fig. 7.

According to Table II, the silicon consumption decreases rapidly at the SiH<sub>4</sub> flow rate of 9 sccm. Figure 9 shows the influence of SiH<sub>4</sub> flow rates on the difference in the thickness of silicide on silicon and on SiO<sub>2</sub>. The difference increases, reaches a peak, and then decreases rapidly

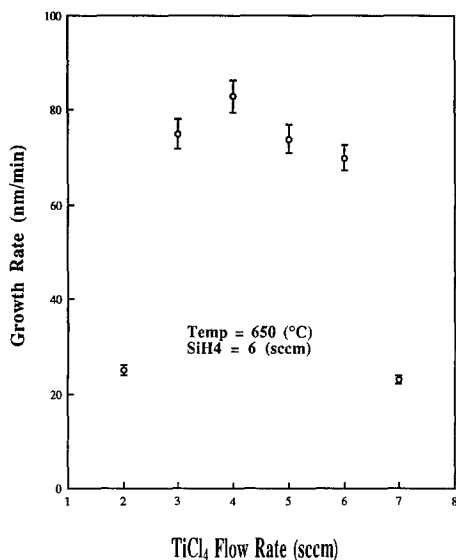


Fig. 7. The average growth rate of silicide vs. TiCl<sub>4</sub> flow rates for a deposition time of 3 min, a SiH<sub>4</sub> flow rate of 6 sccm, 650°C, and 5 W.

Table II. The depth of silicon consumption as a function of SiH<sub>4</sub> flow rates for a constant TiCl<sub>4</sub> flow rate of 4 sccm.

SiH <sub>4</sub> flow rate (sccm)	Depth of Si consumption (nm)
6	350-550
9	<10

when the gas flow rate is 9 sccm. The increase in the difference is attributable to more solid silicon participation in the silicide formation. The rapid decrease is due to a decrease in silicon consumption, as shown by Table II. Therefore, silane seems to have two different effects on silicide formation depending on silane gas flow rates: Enhancing solid silicon reaction with TiCl<sub>4</sub>; and suppression of silicon consumption.

*Blanket silicide with no Si consumption.*—XTEM of a silicide deposited at 590°C with a gas flow ratio (SiH<sub>4</sub>/TiCl<sub>4</sub>) of 8/4 (sccm) shows a conformal step coverage and no Si consumption from the substrate (see Fig. 10). This silicide film with no silicon consumption has promising applications to shallow junction contacts as well as via hole fillings.

### Extended Discussion

*Deposition chemistry.*—In the reactor system used here, neutral species can be regarded as dominant species for film growth because ion bombardment effects can be expected to be minimal. Therefore, we propose here possible reactions based on thermodynamic calculations and by-

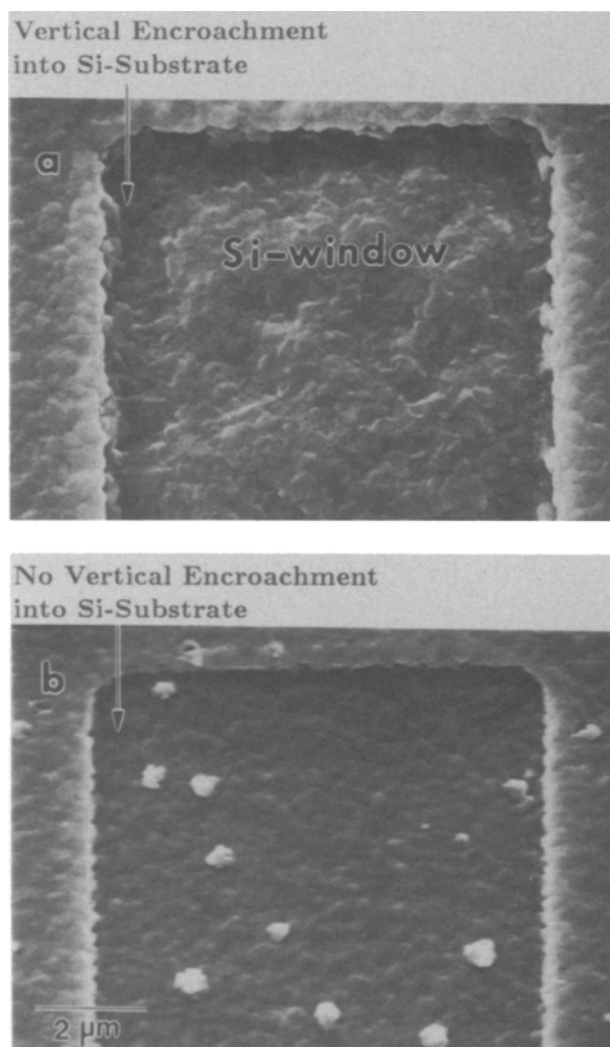


Fig. 8. SEM of titanium silicide deposited on an oxide patterned wafer for 3 min, at 650°C, 5 W and SiH<sub>4</sub>/TiCl<sub>4</sub> flow rate ratio of (a) 6/4, (b) 9/4 (sccm).

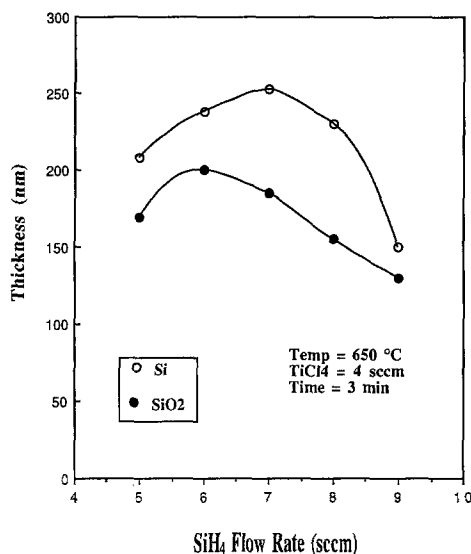
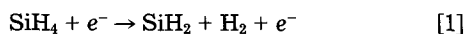


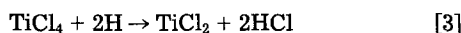
Fig. 9. The effects of SiH<sub>4</sub> flow rates on the difference of the thickness of titanium silicide deposited on silicon and SiO<sub>2</sub> for a constant TiCl<sub>4</sub> flow rate of 4 sccm, 650°C, and 5 W.

product-gases detected by a QMS. Thermodynamic calculation was used to predict the possible reaction for surface reactions based on the assumptions that equilibrium condition was maintained between gas species and adsorbed species, and ion bombardment on the surface could be neglected. The formation of stable TiSi<sub>2</sub> and the mass transport limited region may make two assumptions reasonable.

Our QMS detects a rapid increase in H<sub>2</sub> soon after striking the plasma, which suggests that the following reaction in the gas phase may be dominant



The generated atomic hydrogen radicals may react with TiCl<sub>4</sub> to produce TiCl<sub>2</sub> and HCl gases through reaction [3]



In addition, the generated silylene (SiH<sub>2</sub>) suggests that reaction [4] may be expected



Reaction [4] is consistent with the QMS detection of more SiH<sub>4</sub>Cl and less HCl with increasing silane gas flow rate.

The following silicon-chlorine-hydrogen by-products were detected during the silicide deposition: H<sub>2</sub>, HCl, SiH<sub>3</sub>Cl, SiCl, SiH<sub>2</sub>Cl<sub>2</sub>, and SiCl<sub>2</sub>. SiCl<sub>4</sub> and TiCl<sub>4</sub> were not detected during the deposition in this system, maybe because heavy weight molecules experience more transmission losses in a quadrupole mass filter than lighter ones. Also, heavy weight molecules cannot be sufficiently col-

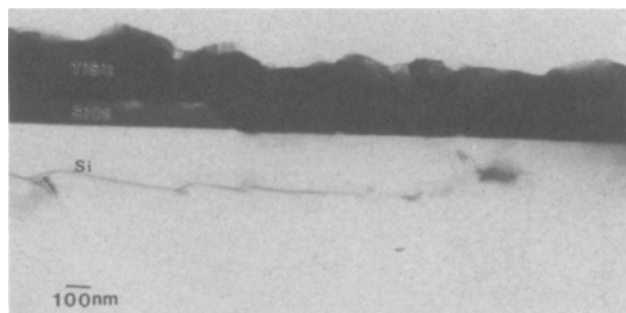
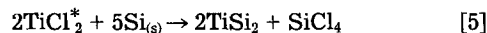


Fig. 10. Cross-sectional TEM of blanket titanium silicide deposited on an oxide patterned wafer for 5 min, at 590°C, SiH<sub>4</sub>/TiCl<sub>4</sub> flow ratio of 8/4 (sccm), and 5 W.

lected through a bypass line having a small diameter hole in the ionization chamber (12). SiCl and SiCl<sub>2</sub> signals were interpreted here as the decomposition of SiCl<sub>4</sub>. Based on this interpretation and the detection of SiH<sub>4</sub>Cl, we propose reaction [5] for silicide formation due to silicon diffusion across silicide layer and reaction [6] for silicon etching.

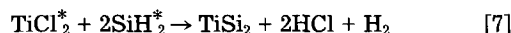
*Silicide formation due to solid silicon.*—



where \* notes adsorbed state of gas species on a surface.

Based on the standard free energy change, both reactions are thermodynamically favorable. Reaction [6] is more thermodynamically favorable than reaction [5], consistent with Fig. 2(c), which suggests that a small fraction of silicon from the substrate contributed to the silicide formation. TiCl<sub>2</sub> may react with SiH<sub>2</sub> to form TiSi<sub>2</sub> through reaction [7].

*Silicide formation due to silane reaction.*—



where \* notes adsorbed state of gas species on a surface.

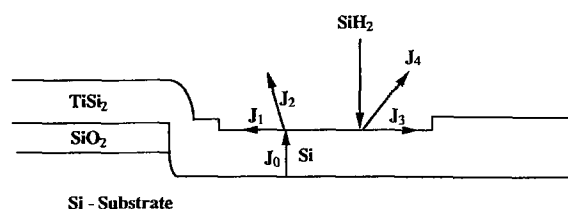
Therefore, increasing the silane gas flow rate increases the forward reaction of reactions [7] and [8], and also retards the surface reaction of silicon, especially silicon etching reaction [6], because of consumption of HCl available to reaction [6] through reactions [4] and [8].

From these considerations, silicon consumption should be a strong function of the gas composition as well as the temperature.

*Kinetic model of silicon consumption.*—The kinetic model proposed to explain the effects of the SiH<sub>4</sub> gas flow rates on silicon consumption is confirmed by the results for thin silicides (≤3000 Å). Figure 11 is a schematic representation of the process of silicon consumption as well as silane reaction. Silicon consumption can be modeled as a sequence of two events; silicon diffusion across a silicide layer; and surface reaction of solid silicon including silicide formation (displacement reaction) and silicon etching. We do not include the evaporation of silicon atoms because the vapor pressure of silicon is very low at our temperatures (13). The flux of silicon across the silicide can be expressed as

$$J_0 = D_0 \exp\left(\frac{-Q_0}{kT}\right) \frac{\partial[\text{Si}]}{\partial x} \quad [9]$$

where  $J_0$  is the diffusion flux of silicon across silicide layer,  $Q_0$  is the activation energy for silicon diffusion, and  $[\text{Si}]$  is



Si - Substrate

### Proposed Reactions

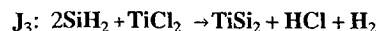
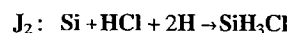
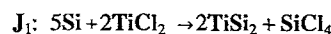


Fig. 11. Schematic representation of the process of silicon consumption and silane reaction.

the concentration of silicon. The flux of surface reaction of solid silicon can be expressed in two parallel ways

$$J_1 = K_1^0 \exp \frac{-Q_1}{kT} [\text{Si}][\text{HCl}][\text{H}]^2 \quad [10]$$

$$J_2 = K_2^0 \exp \frac{-Q_2}{kT} [\text{Si}]^5 [\text{TiCl}_2]^2 \quad [11]$$

where  $J_1$  is the flux of silicon for silicon etching,  $J_2$  is for silicide formation,  $Q_1$  is the activation energy for silicon etching,  $Q_2$  is for silicide formation, and  $[ ]$  is the concentration of each species on the surface. We assume steady state condition during silicon consumption, so the silicon flux can be expressed as

$$J_{\text{si}} = J_0 = J_1 + J_2 \quad [12]$$

According to Eq. [12], the silicon consumption is limited by either silicon diffusion across the silicide ( $J_0$ ), or surface reaction of solid silicon on the surface ( $J_1$  and  $J_2$ ). If the mass transport of silicon across silicide limits the silicon consumption, the silicon consumption is not dependent on gas composition. However, Fig. 10 reveals that increasing silane gas flow rate decreases the silicon consumption, which suggests that the silicon consumption is controlled not by the mass transport of silicon across the silicide layer, but by the surface reaction of silicon on the surface for silicide less than 3000 Å.

Figure 9 shows that the difference between the thickness of silicide on silicon window and that on  $\text{SiO}_2$  increases and reaches a peak when the silane gas flow rate is 7 sccm. This suggests that silicon diffusing from the substrate is participating more in the formation of silicide as the silane gas flow rate is increased. Increasing  $\text{SiH}_4$  flow rates increases the forward reaction of Eq. [1]. Increased  $\text{SiH}_2$  favors the forward reaction of Eq. [4]. As a result, the consumption of HCl is increased. Increasing silane gas flow rate enhances a surface reaction path of silicon to silicide formation, while suppressing silicon etching of Eq. [6] due to the consumption of HCl. Therefore, the gas composition may decide the surface reaction path of silicon either to silicide formation or to silicon etching with different activation energies by influencing the concentration of HCl.

In addition to the dependence of  $\text{SiH}_4$  flow rate on the surface reaction of silicon, the reaction of silicon with  $\text{TiCl}_2$ , at high  $\text{SiH}_4$  flow rates, competes with the reaction of  $\text{SiH}_2$  with  $\text{TiCl}_2$ . Table II reveals that the silicon consumption rate at 9 sccm of  $\text{SiH}_4$  flow rate is much lower than that at 6 sccm. This suggests that increasing silane gas flow rate increases the forward reaction of Eq. [7] while retarding the displacement reaction of silicon, thus leading to low consumption of silicon. From this consideration, it is evident that high silane flow rate effectively suppresses the silicon consumption. However, maximum silane gas flow rate is limited because of whisker formation.

### Summary

A cold-wall PECVD system has been used to investigate the effects of variable conditions on the growth of titanium disilicide and on silicon consumption by utilizing the large deposition variable space available with PECVD.

The use of plasma with minimal ion bombardment on the surface enabled the deposition of C54  $\text{TiSi}_2$  at the low temperature of 590°C.

The deposition rates were divided into two distinct regions depending on the temperatures: at the temperature range of 580 to 600°C, the reaction was controlled by sur-

face reaction; at the high temperature above 600°C, it was controlled by mass transfer of gases. The thicknesses of silicides deposited at 650°C both on Si and on  $\text{SiO}_2$  increased approximately proportionally with deposition times, indicating that the reaction was limited by gas transfer, not by solid diffusion across the silicide layer. XTEM of the silicide deposited at 650°C and  $\text{SiH}_4/\text{TiCl}_4$  of 6/4 (sccm), revealed that silane seemed to be a main contributor to silicide formation, and solid silicon a minor contributor in temperature Region 2.

The growth rate was strongly influenced by  $\text{SiH}_4$  and  $\text{TiCl}_4$  flow rates at 650°C. As  $\text{SiH}_4$  was increased, the growth rate increased and then decreased. With increasing  $\text{TiCl}_4$ , a similar trend in the growth rates was observed. Both reactants seemed to be limiting sources to silicide formation so that the maximum growth rate was obtained at the optimum gas ratio under the equilibrium conditions existing between the gas species in the gas and on the surface.

The difference in thickness of silicide on silicon and on  $\text{SiO}_2$  increased as the temperature increased. It was attributable to the enhanced silicon diffusion through the silicide layer with increasing the temperature. The difference was also influenced by the  $\text{SiH}_4$  flow rates. The difference increased and reached a peak when the  $\text{SiH}_4$  flow rate was 7 sccm. The increase may be due to the retarding of silicon etching on the surface.

Silicon consumption rapidly decreased from 4500 to less than 100 Å when the silane gas flow rate increased from 6 to 9 sccm for the constant  $\text{TiCl}_4$  flow rate of 4 sccm at 650°C. A conformal silicide with no silicon consumption was deposited at 590°C, and 8/4 (sccm) of  $\text{SiH}_4/\text{TiCl}_4$  flow ratio. Both results confirmed the strong effects of temperature and silane gas flow rate on silicon consumption.

The proposed kinetic model of silicon consumption and possible reactions provide a qualitative description of the effects of the silane gas flow rate on silicon consumption, indicating why low deposition temperature as well as high gas flow ratio of  $\text{SiH}_4:\text{TiCl}_4$  is effective in suppressing silicon consumption.

Manuscript submitted Oct. 8, 1990; revised manuscript received Dec. 27, 1991.

Massachusetts Institute of Technology assisted in meeting the publication costs of this article.

### REFERENCES

1. K. Shenai, P. A. Piacente, and B. J. Baliga, in "First International Symposium on Advanced Materials for ULSI," M. Scott, Y. Akasaka, and R. Reif, Editors, PV 88-19, p. 155, The Electrochemical Society Soft-bound Proceedings Series, Pennington, NJ (1989).
2. P. Tedrow, V. Ilderem, and R. Reif, *Appl. Phys. Lett.*, **46**, 189 (1985).
3. V. Ilderem and R. Reif, *ibid.*, **53**, 687 (1988).
4. V. Ilderem and R. Reif, *This Journal*, **135**, 2590 (1988).
5. C. Valhas, G. Baret, J. F. Million-Brodaz, C. Bernard, and R. Madar, in "Proceedings of the Sixth European Conference on Chemical Vapor Deposition," R. Porat, Editor, p. 255 (1987).
6. G. J. Reynolds, C. B. Cooper III, and P. J. Gaczi, *J. Appl. Phys.*, **65**, 14 (1989).
7. J. G. Lee and R. Reif, *This Journal*, **139**, 1166 (1992).
8. M. J. H. Kemper, S. W. Woo, and F. Huizinga, Abstract 377, p. 533, The Electrochemical Society Extended Abstracts, Vol. 84-2, New Orleans, LA, Oct. 7-12, 1984.
9. M. Tabe, *Appl. Phys. Lett.*, **45**, 1073 (1984).
10. T. R. Yew and R. Reif, *J. Appl. Phys.*, **68**, 4681 (1990).
11. F. Y. Robb, *This Journal*, **131**, 2906 (1984).
12. J. F. O'Hanlon, "A User's Guide to Vacuum Technology," p. 73, Wiley and Sons, New York (1980).
13. *Ibid.*, p. 372.